forum acusticum 2026
8-12 September · Graz, Austria

EQUIVALENT SOUNDBOARD FOR PIANO MODEL

Dóra Jenei-Kulcsár[1], Péter Fiala[1]

[1] *Department of Networked Systems and Services, Faculty of Electrical Engineering and Informatics, Budapest University of Technology and Economics, Műegyetem rkp. 3., H-1111 Budapest, Hungary.*

This paper is a revised version of the authors' submitted manuscript that was peer-reviewed by at least two anonymous reviewers.

Abstract

This paper investigates the substitution of traditional ribbed piano soundboards with an equivalent single-ply structure while preserving key acoustical and mechanical characteristics. Piano soundboards play a crucial role in sound radiation, inter-string coupling, and overall tonal quality, all of which are strongly influenced by geometry and material properties. With the decreasing availability of high-quality tonewood and increasing interest in sustainable and cost-effective alternatives, engineered materials and optimized design methods are gaining importance.

Building on prior findings that sound quality can be described through quantitative indicators linked to soundboard admittance and modal behavior, this work focuses on replicating these properties in a simplified structure. A two-step estimation approach is applied: first, ribs are replaced by an equivalent transversely isotropic layer, and second, the effective properties of the resulting laminate are determined.

The proposed method systematically derives a single-ply equivalent model and evaluates its performance through modal analysis and admittance comparison. Although the resulting parameters are hypothetical and not yet validated for physical realization, the study yields to offer a conceptual framework for future development of alternative piano soundboard designs.

Keywords: *piano soundboard, physics-based sound synthesis, modal description, estimated mechanical properties*

1. Introduction

Understanding the piano soundboard is a key element in the mechanical and acoustical modeling of the piano. The geometry and material properties affect the sound quality through inter-string coupling and sound radiation. The mechanical and material properties determine the available dynamic range and coloring of the produced sound. Not only the proper construction but also the carefully selected and processed materials guarantee the instrument's reliability and durability. The current soundboard model is designed as part of an abstract piano model that covers the process from hammer strike to radiated sound. The soundboard's behavior is modeled using a filter set parameterized by the soundboard's modal description (eigenfrequencies, mode shapes, and damping).

Piano soundboards are complex structures in which the main resonator is stiffened and slightly bowed with ribs on the bottom, while on the upper side, bridges are installed. The ribs not only reduce the strong in-plane anisotropy caused by the wood grain direction, but also contribute to the formation of the soundboard's 'crown', which helps to support the load of the strings. The main resonator is traditionally built from solid tonewood, especially spruce, but experimentation with it is as old as the instrument itself. Nowadays, engineered materials are emerging for several reasons. The question is whether it is possible to reproduce the same – or at least quite similar – vibroacoustic characteristics of the original soundboard using an equivalent structural model.

It has been previously shown that the modal description determines the admittance of the soundboard, serving as a fundamental component in modeling the dynamic termination of strings, including coupling effects, losses, and reflections. Because this also determines the surface velocities used to model sound radiation, it directly influences the final characteristics of the radiated sound (e.g. [1], [2]).

Since the modal properties are determined by the system matrix – dependent on both material parameters and geometric configuration, as discussed in sections 2.3–2.5 – it follows that different material-geometry combinations may result in equivalent (or at least similar) system matrices.

This fact motivates the investigation of alternative structural designs. It suggests that a traditional ribbed soundboard may be effectively substituted (at least for simulation purposes) by a single-ply configu-

Corresponding author: *dkulcsar@hit.bme.hu.*

ration.
The modal behavior of traditional piano soundboards has been extensively studied (e.g. [3], [4], [5], [6]). Numerous studies have proposed various approaches for modeling piano soundboards based on measurement results (e.g. [4], [7], [8], [9], [10], [11]). The used material properties and modeling techniques of woods are well documented (e.g. [8], [12], [13]).
In the present work, an attempt is made to substitute the traditional piano soundboard with a single-ply construct, so that the modal properties and admittance of the resulting soundboard meet the original ones as closely as possible. For this, estimation methods are applied. In the first step, ribs are substituted by a transversely isotropic stiffening layer, implementing the proposed estimation method for an equivalent stiffening layer to substitute equidistant ribbed structures in [14]. To determine the longitudinal direction during estimation other than 0°, the concept described in [15] is adapted. In the second step, the effective properties of this two-ply laminate are determined. Determination of effective mechanical properties of laminar composites is widely documented (e.g. [16], [17], [18], [19]).
The estimation results are discussed in terms of modal description and admittance. It is noted that in the case of the current research, the resulting parameters should be considered hypothetical. There is no ongoing investigation into the research of the material realization, stability, durability, or the static feasibility aspects of the resulting digital model. It is intended more as a thought-provoking work, with a possibility of future development. The results are demonstrated on an abstract example.
In the following sections, we briefly introduce a general ribbed soundboard model and the step-by-step estimation, and present some numerical simulation results.

2. Model Overview

2.1. Mechanical Properties

Wood is generally modeled as an orthotropic material, defined by three unique and independent mechanical properties along three mutually perpendicular axes. These axes are aligned with the longitudinal axis parallel to the grain (fiber), the radial axis normal to the growth rings, and the tangential axis perpendicular to the grain but tangent to the growth rings. [20]
Since the length and width of the soundboard far exceed its thickness, the thin plate assumption and 2D-orthogonality can be applied to it with isotropic properties in the 2-3 plane. Dominant longitudinal behavior in the case of the ribs allows further simplification, reducing the modeling to isotropic materials.
Spruce – particularly Norway or Sitka spruce – is the preferred material for high-quality piano soundboards. Typical 2D material properties of it are detailed in Table 1, including density ρ, Young's moduli E_i, Poisson's ratio ν_ij and shear moduli G_ij) (s.a. [8], [12], [13], [20])

Table 1: Typical Mechanical Properties of Spruce

Property	Metric	Min.	Avg.	Max.
ρ	kg m^{-3}	380	410	440
E_1	GPa	10	12.95	15.9
E_2	GPa	0.47	0.685	0.9
ν_{12}	1	0.26	0.35	0.44
G_{12}	GPa	0.72	0.96	1.2

2.2. The Material Matrix

The material model is based on the generalized Hooke's law:

$$\hat{\sigma}_\mathrm{ij} = \sum_{k=1}^{3}\sum_{l=1}^{3} \hat{\mathrm{D}}_\mathrm{ijkl} \cdot \hat{\varepsilon}_\mathrm{kl}, \tag{1}$$

where $\hat{\sigma}_\mathrm{ij}$, $\hat{\varepsilon}_\mathrm{kl}$, and $\hat{\mathrm{D}}_\mathrm{ijkl}$ represent components of the stress, strain, and material[1] tensors, respectively. Due to symmetry of the stress and strain tensors – adopting the Voigt matrix notation (with index order: $\hat{\sigma}_{11}$, $\hat{\sigma}_{22}$, $\hat{\sigma}_{33}$, $\hat{\tau}_{23}$, $\hat{\tau}_{31}$, $\hat{\tau}_{12}$) – the material tensor is reduced to a 6×6 symmetric matrix $\hat{\mathbf{D}}$. The elements of the material matrix[2] can be derived from mechanical properties (E_i, ν_ij, G_ij) and it is well-documented in the literature. To compute forces and moments, the material matrix must be reordered to separate the membrane ($\mathbf{m}$ for 1, 2, 6 indices) and transverse shear ($\mathbf{s}$ for 3, 4, 5 indices) stiffness components. This results in 2×2 block-diagonal matrix ($\hat{\mathbf{D}}^\mathbf{ms}$) containing symmetric 3×3 sub-matrices ($\hat{\mathbf{D}}^\mathbf{m}$ and $\hat{\mathbf{D}}^\mathbf{s}$).
Because of the thin plate assumption in our specific case, this matrix can be further simplified: since $\hat{\sigma}_{33}$-component of the stress vector is negligible (in fact for plane stress condition by definition zero), the first row and column of the matrix $\hat{\mathbf{D}}^\mathbf{s}$ are set to zero, corresponding to a vanishing strain component $\hat{\varepsilon}_{33}$. Due to longitudinal dominance, components ε_{22}, γ_{23}, σ_{22} and τ_{23} are also negligible in the ribs, leading to zero second rows and columns in both sub-matrices.
To determine the applied material matrix[3] ($\mathbf{D}^\mathbf{ms}$), a transformation

$$\mathbf{D}^\mathbf{ms} = \mathbf{T}^\mathbf{ms}_{\boldsymbol{\sigma}} \cdot \hat{\mathbf{D}}^\mathbf{ms} \cdot \mathbf{T}^\mathbf{ms}_{\boldsymbol{\varepsilon}} \tag{2}$$

from the material basis to the reference basis of the geometry must be performed [14], which requires defining the fiber orientation for both the plate (θ_p) and the ribs (θ_s).

2.3. The System Matrix

To determine the effective stiffness properties of an arbitrary, unidirectional, eccentric stiffened composite laminate, the system matrix[4] ($\mathfrak{D}$) must be determined. This matrix relates mid-plane strains ($\boldsymbol{\varepsilon}_\mathbf{0}$) and curvatures ($\boldsymbol{\kappa}$) to the resultant forces and moments,

[1]stiffness tensor
[2]stiffness matrix or material constitutive matrix
[3]transformed stiffness/constitutive matrix
[4]laminate constitutive matrix

reducing the complex 3D stacking sequence to a 2D laminate representation. The forces ($\mathbf{N}$) and moments ($\mathbf{M}$) can be determined independently for membrane and transverse shear components (s.a. [14]). In most practical applications, transverse shear forces and moments are very small and so negligible. Although they could be significant for some asymmetric laminates, basically the material equation without the shear components is applied and corrected (when needed) (s.a. [17]):

$$\begin{pmatrix} \mathbf{N} \\ \mathbf{M^b} \end{pmatrix} = \begin{pmatrix} \mathbf{A} & \mathbf{B} \\ \mathbf{B} & \mathbf{D_b} \end{pmatrix} \cdot \begin{pmatrix} \boldsymbol{\varepsilon_0} \\ \boldsymbol{\kappa} \end{pmatrix} = \boldsymbol{\mathfrak{D}} \cdot \begin{pmatrix} \boldsymbol{\varepsilon_0} \\ \boldsymbol{\kappa} \end{pmatrix}. \tag{3}$$

For any kind of ribbed plate (a laminate with L plies holding stiffeners with R sections), this computation can be carried out ply- and section-wise. The resulting extensional ($\mathbf{A}$), coupling ($\mathbf{B}$) and bending ($\mathbf{D_b}$) stiffness matrices combining plate and stiffeners effects:

$$\mathbf{A} = \mathbf{A_{plate}} + \mathbf{A_{ribs}} = \sum_{k=1}^{L+R} \mathbf{D}^{\mathbf{m}}_{\mathrm{k}} \cdot (z_{\mathrm{k}} - z_{\mathrm{k}-1}), \tag{4}$$

$$\mathbf{B} = \mathbf{B_{plate}} + \mathbf{B_{ribs}} = \sum_{k=1}^{L+R} \frac{1}{2} \cdot \mathbf{D}^{\mathbf{m}}_{\mathrm{k}} \cdot \left(z_{\mathrm{k}}^2 - z_{\mathrm{k}-1}^2\right), \tag{5}$$

$$\mathbf{D_b} = \mathbf{D_{b_{plate}}} + \mathbf{D_{b_{ribs}}} = \sum_{k=1}^{L+R} \frac{1}{3} \cdot \mathbf{D}^{\mathbf{m}}_{\mathrm{k}} \cdot \left(z_{\mathrm{k}}^3 - z_{\mathrm{k}-1}^3\right). \tag{6}$$

The matrices in Eqq. (4)-(6) depend only on the material matrices $\mathbf{D}^{\mathbf{m}}_{\mathrm{k}}$ and the vertical coordinates z_{k}, which are defined relative to the board's neutral plane (z_{N}, $z_0 = -z_{\mathrm{N}}$). For the traditional soundboard model (made of solid wood with rectangular ribs) $L = 1$ and $R = 1$ is assumed.

2.4. The Equation of Motion

The dynamics of a general elastic volume of an arbitrary boundary, composed of a Kelvin-Voigt material, is governed by the following equation (balance of linear momentum):

$$\boldsymbol{\mathcal{S}}^{\mathrm{T}} \cdot \boldsymbol{\sigma} \cdot \mathbf{b} = \rho \cdot \frac{\partial^2 \mathbf{u}}{\partial t^2}, \tag{7}$$

where $\boldsymbol{\mathcal{S}}^{\mathrm{T}} \cdot \boldsymbol{\sigma}$ represents the divergence of the stress vector, incorporating frequency-dependent damping via the matrix $\boldsymbol{\mathcal{H}}$ in formulation of the stress vector: $\boldsymbol{\sigma} = \boldsymbol{\mathfrak{D}} \cdot \boldsymbol{\varepsilon} + \boldsymbol{\mathcal{H}} \cdot \frac{\partial \boldsymbol{\varepsilon}}{\partial t}$. Here $\mathbf{b}$ denotes body forces, ρ is the density and $\mathbf{u}$ represents the displacement field (s.a. [21]).

For the specific application of soundboard – a stiffened thin plate with ribs and bridges on separate sides – it is assumed that the displacement $\mathbf{u}$ follows the Kirchhoff-Love theorem, so the governing equation Eq. (7) can be rewritten as

$$\boldsymbol{\mathcal{S}}^{\mathrm{T}} \cdot \boldsymbol{\mathfrak{D}} \cdot \boldsymbol{\mathcal{S}} \cdot \mathbf{u} + \boldsymbol{\mathcal{H}} \cdot \frac{\partial \mathbf{u}}{\partial t} + \mathbf{b} = \rho \cdot \frac{\partial^2 \mathbf{u}}{\partial t^2}. \tag{8}$$

The goal is to solve the weak formulation of Eq. (8) using the finite element method: The exact solution for displacement is approximated using a finite number of polynomial base functions ($\boldsymbol{\mathcal{N}}$) over the discretized geometry. This results in the so-called mass and stiffness matrices ($\boldsymbol{\mathcal{M}}$, $\boldsymbol{\mathcal{K}}$). The damping coefficients in matrix $\boldsymbol{\mathcal{H}}$ are modeled based on Rayleigh's method as a linear combination of $\boldsymbol{\mathcal{M}}$ and $\boldsymbol{\mathcal{K}}$, or are simply set based on engineering appraisals (s.a.[22], [23]). To improve computational efficiency, the master-slave multi-freedom constraint theory is applied, treating the plate as the master geometry and the ribs and bridges as slave geometries (reducing the size of $\boldsymbol{\mathcal{M}}$ and $\boldsymbol{\mathcal{K}}$) (e.g. [24]).

2.5. The Modal Description

The differential equation equivalent to the weak formulation of Eq. (8) is

$$\boldsymbol{\mathcal{K}} \cdot u(\mathbf{x}, t) + \boldsymbol{\mathcal{H}} \cdot \frac{\partial u(\mathbf{x}, t)}{\partial t} + \boldsymbol{\mathcal{M}} \cdot \frac{\partial^2 u(\mathbf{x}, t)}{\partial t^2} = f(\mathbf{x}, t), \tag{9}$$

where $u(\mathbf{x}, t)$ denotes the space- and time-dependent displacement. To find the free vibration modes, the damping matrix and the external force f are set to zero. After transforming to the frequency domain, the eigenfrequencies (ω_{k} and mode shapes (Φ_{k})) are determined by solving the generalized eigenvalue problem:

$$\left(\boldsymbol{\mathcal{K}} - \omega^2 \cdot \boldsymbol{\mathcal{M}}\right) \cdot U(\mathbf{x}, \omega) = 0. \tag{10}$$

The displacement is then expressed as a superposition of these modes:

$$U(\mathbf{x}, \omega) = \sum_{k=1}^{n} \Phi_{\mathrm{k}}(\mathbf{x}) \cdot \mathfrak{A}_{\mathrm{k}}(\omega). \tag{11}$$

3. Estimation of Mechanical Properties

From a structural modeling perspective, piano soundboards have 'arbitrary' (although systematically but not equidistant) placed stiffeners. To represent them with an equivalent stiffening layer, they must be transformed into an equidistant rib structure. In this study, the mean thickness of the plate (t) and the mean dimensions (height (h), width (w), and distance (d)) of the ribs are used, while the original material properties are preserved.

To determine the structural response, the 3×3 stiffness matrices $\mathbf{A}$, $\mathbf{B}$, $\mathbf{D_b}$ from Eq. (3) must be defined. For a solid 2D-orthotropic plate, the constitutive relationship is given by the inverse of the material matrix:

$$\hat{\mathbf{D}}^{\mathbf{m}^{-1}} = \begin{pmatrix} \frac{1}{E_1} & -\frac{\nu_{12}}{E_1} & 0 \\ -\frac{\nu_{12}}{E_1} & \frac{1}{E_2} & 0 \\ 0 & 0 & \frac{1}{G_{12}} \end{pmatrix}. \tag{12}$$

The required stiffness matrices are then computed using Eqq. (4)-(6) and the transformation rules in Eq. (2). For the ribs, these stiffness components are derived in [14]:

$$\hat{\mathbf{A}}_{\mathbf{ribs}} = \begin{pmatrix} \frac{E_1 \cdot h \cdot w}{d} & 0 & 0 \\ 0 & 0 & 0 \\ 0 & 0 & \frac{k_s \cdot G_s \cdot h \cdot w}{4 \cdot d} \end{pmatrix}, \tag{13}$$

$$\hat{\mathbf{B}}_{\mathbf{ribs}} = \left(z_{\mathrm{L}} + \frac{h}{2} \right) \cdot \hat{\mathbf{A}}_{\mathbf{ribs}}, \tag{14}$$

$$\hat{\mathbf{D}}_{\mathbf{b_{ribs}}} = \begin{pmatrix} \frac{E_1 \cdot I_{22}}{d} & 0 & 0 \\ 0 & 0 & 0 \\ 0 & 0 & \frac{G_s \cdot J_s}{4 \cdot d} \end{pmatrix}, \tag{15}$$

where G_s represents the effective shear modulus, k_s the effective shear correction factor, and z_{L} is the vertical position of the plate's top surface (rib base), I_{22} the moment of inertia, and J_s the effective torsional stiffness.

To model the system using an equivalent stiffening layer, instead of ribs, the effective mechanical properties must be estimated. While [25] suggests estimations based on $\mathbf{A}_{\mathbf{ribs}}$, this approach proved insufficient for capturing the required modal behavior in this study. Instead, because the ribs are eccentric to the neutral plane – a factor captured by the inertia and torsional stiffness in $\hat{\mathbf{D}}_{\mathbf{b_{ribs}}}$ – the estimation is derived from the bending stiffness matrix. Assuming the equivalent stiffening layer (esl) shares the same bending stiffness as the ribs, the material matrix $\hat{\mathbf{D}}^{\mathbf{m}}_{\mathbf{esl}}$ is formulated as:

$$\hat{\mathbf{D}}^{\mathbf{m}}_{\mathbf{esl}} \equiv \frac{3}{(z_{\mathrm{L}} + t_s)^3 - z_{\mathrm{L}}^3} \cdot \hat{\mathbf{D}}_{\mathbf{b_{ribs}}}, \tag{16}$$

where the equivalent thickness t_s is determined by the rib geometry to accurately reflect the membrane-dominant modal action [14]:

$$t_s = \frac{h \cdot w}{d}. \tag{17}$$

The estimated effective mechanical properties for the equivalent stiffening layer are extracted from the components of $\hat{\mathbf{D}}^{\mathbf{m}}$ following a similar method as in [15]:

$$\tilde{E}_1 = \hat{D}_{11} - \frac{\hat{D}_{12}^2}{\hat{D}_{22}}, \tag{18}$$

$$\tilde{E}_2 = \hat{D}_{22} - \frac{\hat{D}_{12}^2}{\hat{D}_{11}}, \tag{19}$$

$$\tilde{G}_{12} = \hat{D}_{66}, \tag{20}$$

$$\tilde{\nu}_{12} = \frac{\hat{D}_{12}}{\hat{D}_{22}}. \tag{21}$$

It is noted that the density of the stiffener material remains unaffected by the estimation, and the fiber direction of the estimated stiffening layer set to be parallel to the original ribs; $\tilde{E}_1 = \hat{D}_{11}$, $\tilde{E}_2 \approx 0$, $\tilde{G}_{12} = \hat{D}_{66}$, and $\tilde{\nu}_{12} \approx 0$.

The mechanical properties for the single-ply equivalent bare board (ebb) can be estimated using the bending stiffness matrix, $\mathbf{D_b}$, from Eq. (6). Assuming a symmetric layup relative to the neutral plane, the material stiffness matrix $\hat{\mathbf{D}}^{\mathbf{m}}_{\mathbf{ebb}}$ is calculated as:

$$\hat{\mathbf{D}}^{\mathbf{m}}_{\mathbf{ebb}} \equiv \frac{4}{t_{\mathrm{ebb}}} \cdot \hat{\mathbf{D}}_{\mathbf{b}}, \tag{22}$$

where $t_{\mathrm{EBB}} = t + t_s$ is the total equivalent thickness. Effective mechanical properties are determined using Eqq. (18)-(21). The resulting material retains the density of the original structure, with the fiber direction aligned with the original ribs.

4. Numerical Example

Preliminary simulations were conducted to evaluate the feasibility of the described estimation method. The model output is demonstrated using an abstract geometry. The rectangle soundboard (1×1.5 m) with clamped boundaries has a uniform thickness of 8 mm. Bridges were omitted from this model as they are not planned to be modified in the final structure. The ribs are 2.5 cm wide with a uniform height of 3 cm. The material properties used in the current model are listed in Table 1, assuming isotropic average values. As further abstraction a constant modal damping coefficient of 8% was applied [23] and assumed to be homogeneously distributed across the geometry.
The modes were determined for this abstract construction. The first 50 eigenfrequencies are plotted in Fig. 1. The results show that the eigenfrequencies of the

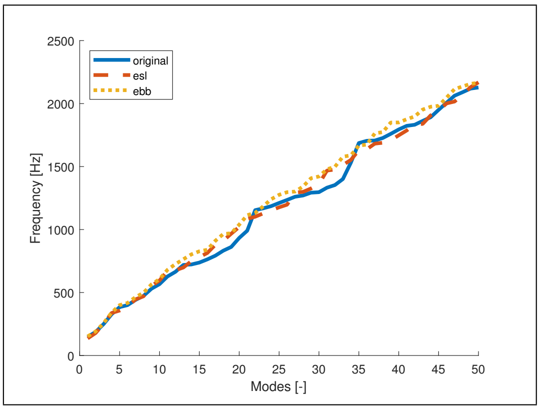

Figure 1: Computed eigenfrequencies: original (solid), equivalent stiffening layer (dashed), equivalent bare board (dotted).

estimated models correlate quite well with the original values for the computed modes; however, deviation can reach or exceed even a whole note (s.a. Fig. 2). While the overall estimation trend in eigenfrequencies is encouraging, the mode shapes also reveal the limitations (Fig. 3). For low-frequency modes, the rib dominance is accurately imitated by carefully setting the fiber direction. Conversely, at higher frequencies, the stiffening and modal localization effects are not

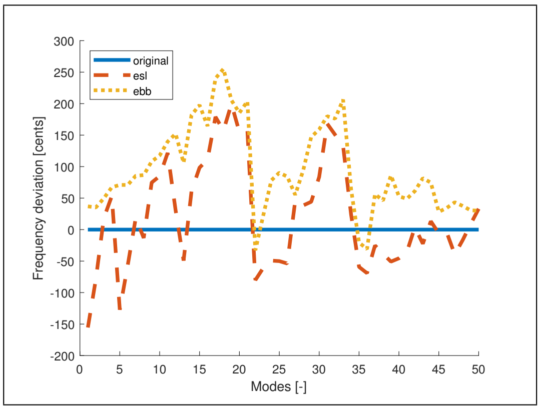

Figure 2: Deviation of computed eigenfrequencies from the original model based on $\Delta = 1200 \cdot \log_2 \frac{f_1}{f_2}$: original (solid), equivalent stiffening layer (dashed), equivalent bare board (dotted).

faithfully captured.

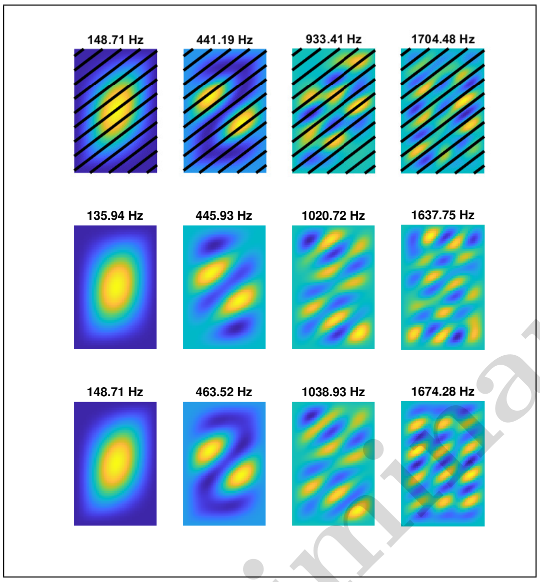

Figure 3: Example modes: original (top), equivalent stiffening layer (middle), equivalent bare board (bottom).

Soundboard driving point admittance (mechanical mobility) was computed near the center of the board ([0.53;0.79] m). An inspection of the initial section of the admittance curve (Fig. 4) shows that while the frequencies and amplitudes of the second modes match well across all models, the first mode exhibits a shift under the equivalent stiffening layer assumption. For subsequent peaks, the magnitude of the variation in pitches and amplitudes is significant for sound modeling applications. A clearly noticeable and measurable change in the coloring and decay is expected (s.a.[2]). Although it must definitely taken into account that this abstract example is not able to reproduce the stiffening effects of bridges, shape, or material orthotropy, all of which are critical factors in an actual piano soundboard.

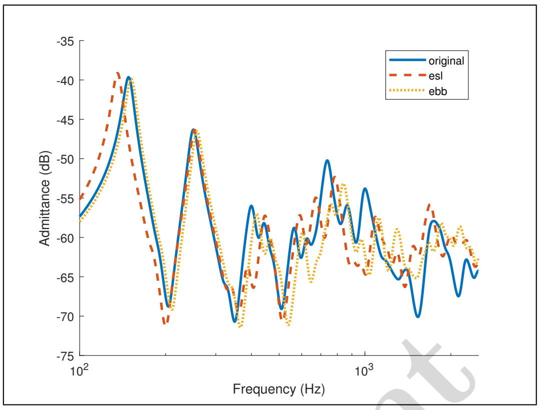

Figure 4: The initial (low frequency) section of the admittance (dB re 1 $\frac{\mathrm{m}}{\mathrm{sN}}$): original (solid), equivalent stiffening layer (dashed), equivalent bare board (dotted).

5. Conclusion

This paper investigated the estimation of possible soundboard substitutes. After a brief introduction with the key elements of the modeling, a possible estimation method was introduced, starting by a traditional ribbed soundboard, substituting the ribs through an equivalent stiffening layer, to a single-ply representation of the original structure. The estimation was demonstrated on an abstract numerical example. Besides all the limitations of the abstract model, there are some positive results of the simulations: The overall trend in eigenfrequencies seems to be estimable quite accurate, and the stiffening effect of the ribs can be recreated for the first modes based on the mode shapes. Based on the admittance and mode shapes, the estimation method needs to be improved to better fit the original soundboard behavior.

References

[1] P. M. Valiente, G. Squicciarini, and D. Thompson, “Modeling the interaction between piano strings and the soundboard,” in *Fourth Vienna Talk on Music Acoustics*, vol. 49, ASA, 2022, p. 035 019. DOI: 10.1121/2.0001685

[2] D. Jenei-Kulcsár and P. Fiala, “Piano soundboard analysis at radiated sound,” *Periodica Polytechnica Electrical Engineering and Computer Science*, vol. 67, no. 3, pp. 291–299, Jul. 2023. DOI: 10.3311/ppee.21181

[3] N. Giordano, “Mechanical impedance of a piano soundboard,” *The Journal of the Acoustical Society of America*, vol. 103, no. 4, p. 2128, Apr. 1998. DOI: 10.1121/1.421358

[4] J. Berthaut, M. Ichchou, and L. Jézéquel, “Piano soundboard: Structural behavior, numerical and experimental study in the modal range,” *Applied*

Acoustics, vol. 64, no. 11, pp. 1113–1136, Nov. 2003. DOI: 10.1016/s0003-682x(03)00065-3

[5] R. Corradi, S. Miccoli, G. Squicciarini, and P. Fazioli, "Modal analysis of a grand piano soundboard at successive manufacturing stages," *Applied Acoustics*, vol. 125, pp. 113–127, Oct. 2017. DOI: 10.1016/j.apacoust.2017.04.010

[6] L. He, Y. Liang, L. Zhang, J. Zhou, R. Wang, and Z. Liu, "Measurement and analysis of the vibration responses of piano soundboards with different structures," *Materials*, vol. 17, no. 5, p. 1004, Feb. 2024, ISSN: 1996-1944. DOI: 10.3390/ma17051004

[7] B. Bank, S. Zambon, and F. Fontana, "A modal-based real-time piano synthesizer," *IEEE Transactions on Audio, Speech, and Language Processing*, vol. 18, no. 4, pp. 809–821, May 2010. DOI: 10.1109/TASL.2010.2040524

[8] X. Boutillon and K. Ege, "Vibroacoustics of the piano soundboard: Reduced models, mobility synthesis, and acoustical radiation regime," *Journal of Sound and Vibration*, vol. 332, no. 18, pp. 4261–4279, Sep. 2013. DOI: 10.1016/j.jsv.2013.03.015

[9] K. Ege and X. Boutillon, "Global and local synthetic descriptions of the piano soundboard," in *Forum Acusticum 2011, Aalborg : Denmark (2011)*, 2011. eprint: arXiv:1210.5109.

[10] J. Chabassier, "Modélisation et simulation numérique d'un piano par modèles physiques," Thèse de doctorat dirigée par Joly, Patrick Mathématiques appliquées Palaiseau, Ecole polytechnique 2012, Ph.D. dissertation, Ecole polytechnique de Paris, 2012, 1 vol. (319 p.)

[11] P. Miranda Valiente, G. Squicciarini, and D. J. Thompson, "Influence of soundboard modelling approaches on piano string vibration," *The Journal of the Acoustical Society of America*, vol. 155, no. 5, pp. 3213–3232, May 2024, ISSN: 0001-4966. DOI: 10.1121/10.0025925

[12] J. Chabassier and M. Durufle, "Physical parameters for piano modeling," Technical Report RT-0425, Apr. 2012, p. 24.

[13] B. Trévisan, K. Ege, and B. Laulagnet, "A modal approach to piano soundboard vibroacoustic behavior," *The Journal of the Acoustical Society of America*, vol. 141, no. 2, pp. 690–709, Feb. 2017. DOI: 10.1121/1.4974860

[14] M. P. Nemeth, "A treatise on equivalent-plate stiffnesses for stiffened laminated-composite plates and plate-like lattices," Langley Research Center, Hampton, Virginia, Tech. Rep., 2011.

[15] O. Zebdi, R. Boukhili, and F. Trochu, "An inverse approach based on laminate theory to calculate the mechanical properties of braided composites," *Journal of Reinforced Plastics and Composites*, vol. 28, no. 23, pp. 2911–2930, Jul. 2008. DOI: 10.1177/0731684408094063

[16] G. Staab, "Laminar composites," in Butterworth-Heinemann, 1999, ch. Laminate Analysis, pp. 191–282, ISBN: 9780750671248.

[17] E. Stein and J. Tessmer, "Theory and computation of multilayer composites," in *Mechanics of Composite Materials and Structures*, C. A. M. Soares, C. M. M. Soares, and M. J. M. Freitas, Eds. Dordrecht: Springer Netherlands, 1999, pp. 369–378, ISBN: 978-94-011-4489-6. DOI: 10.1007/978-94-011-4489-6_24

[18] A. T. Nettles, "Basic mechanics of laminated composite plates," NASA. Marshall Space Flight Center - MSFC, Alabama, Tech. Rep., 1994.

[19] I. Kreja and A. Sabik, "Equivalent single-layer models in deformation analysis of laminated multilayered plates," *Acta Mechanica*, vol. 230, no. 8, pp. 2827–2851, May 2019. DOI: 10.1007/s00707-019-02434-7

[20] R. J. Ross and F. P. L. U. F. Service., "Wood handbook : Wood as an engineering material," Tech. Rep., 2010. DOI: 10.2737/fpl-gtr-190

[21] O. C. Zienkiewicz and R. L. Taylor, *The Finite Element Method for Solid and Structural Mechanics*. Elsevier Science, Aug. 2005, 736 pp.

[22] N. Zabaras and T. Pervez, "Viscous damping approximation of laminated anisotropic composite plates using the finite element method," *Computer Methods in Applied Mechanics and Engineering*, vol. 81, no. 3, pp. 291–316, Aug. 1990. DOI: 10.1016/0045-7825(90)90058-t

[23] J. Göken, S. Fayed, H. Schäfer, and J. Enzenauer, "A study on the correlation between wood moisture and the damping behaviour of the tonewood spruce," *Acta Physica Polonica A*, vol. 133, no. 5, pp. 1241–1260, May 2018. DOI: 10.12693/aphyspola.133.1241

[24] J. Boungard and J. Wackerfuß, "How can the master–slave elimination for multi-point constraints be drastically accelerated?" *PAMM*, vol. 25, no. 4, Dec. 2025, ISSN: 1617-7061. DOI: 10.1002/pamm.70022

[25] F. Danzi, E. Cestino, G. Frulla, and J. M. Gibert, "Equivalent plate model of curvilinear stiffened panels," in *Proc. of the 7th International Conference on Mechanics and Materials in Design Albufeira/Portugal 11-15 June 2017*, J. F. S. Gomes and S. A. Meguid, Eds., INEGI/FEUP, 2017.